Egyptian Geophysical Society
EGS Journal, vol. 7, No. 1, 83-95 (2009)

INTERPRETATION OF AEROMAGNETIC DATA, GABAL ABU MARWA AREA NORTH EASTERN DESERT, EGYPT

M.F. MOUSSA

Geology Department, Faculty of Science, South Valley University, Egypt.

تفسير البيانات المغناطيسية الجوية لجبل أبو مروة شمال الصحراء الشرقية لمصر

الخلاصة: فسرت البيانات المغناطيسية الجوية وبيانات القمر الصناعى لاندسات لتوضيح الاتجاهات التركيبية الغالبة على السطح وتحت السطح لمنطقة الدراسة بالاضافة لتحديد سمك الوحدات الصخرية السطحية وكذلك لتعيين عمق الأجسام المسببة للشاذات المغناطيسية فى منطقة جبل أبو مروة بشمال الصحراء الشرقية لمصر، كذلك أجرى تحليل لإتجاهات الخطوط التركيبية التى اشتقت من خرائط المغناطيسية والقمر الصناعى والجيولوجية للمنطقة وخطوط الصرف التى يغلب عليها الاتجاه شمال شرق-جنوب غرب بينما إتجاهات شمال-جنوب و شرق-غرب تمثل إتجاهات ثانوية.

و أظهر التحليل الأحصائى علاقات قوية متباينة للبيانات المختلفة المستخدمة كما تم تطبيق طريقتين لتحديد الأعماق للشاذات المغناطيسية وهما تحليل البصمة والعدد الموجى المحلى على شبكية البيانات المغناطيسية للشدة الكلية وتم استخدام النتائج المتحصل عليها لرسم خرائط كنتورية للاعماق وقد أوضحت هذه الخرائط أن الأجسام المسببة للشاذات المغناطيسية أو القريبة من السطح متجهه ناحية الجزء الغربى لمنطقة الدراسة بينما توجد قيم لأعماق كبيرة ناحية الجزء الأوسط من منطقة الدراسة وتشكل هذه القيمة حوضاً وجهته الاتجاه شمال غرب -جنوب شرق موازيا للبحر الأحمر وتم عمل نمذجة لاثنين وأربعين بروفيلاً مغناطيسياً لتعيين قيم المعاملات للصخور مثل الحساسية المغناطيسية والعمق والاتساع كما أن هذه النماذج توضح التوزيع تحت السطحى للصخور وعلاقتها بالجيولوجيا السطحية كما أن الوحدات الصخرية السطحية لها حساسية مغناطيسية تتراوح ما بين ٠,٠٠٠٠٠١ إلى ٠,٠٠٧٢ وحدة واتساع يتراوح ما بين ١٠٠ متر إلى ٧٠٠ متر وكذلك لها أعماق محدودة وأن أعماق الأجسام المسببة للشاذات المغناطيسية يبدأ من السطح إلى ١٤٠٠ متر.

ABSTRACT: *Aeromagnetic and landsat data were interpreted to infer the most pronounced tectonic trends, both on the surface and at the subsurface and to determine the thickness of the surface geologic rock units as presently mapped, as well as to estimate the depth to the top of source magnetic bodies in Gabal Abu Marwa area, north Eastern Desert of Egypt. Trend analysis was carried out on the structural lineaments that are deduced from magnetic, shaded relief images and geological map of the study area. Both magnetic and landsat image lineaments revealed four major sets of structural lineaments trending in the NE -SW, NW-SE, N-S and E –W directions. The traced drainage lineaments show major sets trending in the NE- SW direction meanwhile; N-S and E-W directions are observed as secondary lineaments. The statistical test analyses revealed diversity in the correlation strength between the various data sets. Two depth estimation techniques (analytic signal and local wavenumber) were applied on the entire grid of the total-intensity magnetic data. The obtained depth results are used to construct depth contour maps to the top of source bodies. These maps reflect the outcropping or near-surface causative bodies at the central western part of the study area. Meanwhile, a remarkable increase in the depth values toward the central part of the area forming a basin of a NW-SE direction parallel to the Red Sea. This means that the magnetic anomalies are due to relatively deep causative bodies. Forty two magnetic profiles were selected in the modeling process to determine the parameters (susceptibility, depth and width) values of the rock units. These models manifest the subsurface distributions of the rock units and their relation to the surface geology. The surface rock units have susceptibility values ranging from 0.000001 cgs to 0.0072 cgs unit and width values ranging from 100 to 7000 m. However, they have limited depth extension and the depth to the magnetic source bodies starting from the surface to a depth of about 1400 m.*

INTRODUCTION

The study area is located in the north Eastern Desert of Egypt, which is bounded by latitudes 27º 15´ & 27º 43´ 44″ N and longitudes 33º 0` & 33º 41´ 24″E (Fig. 1). It is covered by Precambrian igneous and metamorphic rocks overlain by sedimentary rock units of Cretaceous and Tertiary age. These rock exposures are traversed by several wadis (dry valleys) filled by Quaternary sediments.

The study area shows a special importance, as it is located on the western coast of the Gulf of Suez that is considered the main hydrocarbon province in Egypt. Magnetic method is an effective low coast way to provide valuable information mainly for delineation of subsurface structures and reach better understanding of the basement rocks and their relation to the overlying sedimentary section. The aeromagnetic data used here were surveyed by the Western Geophysical Company of America in 1983. Flight lines were flown in the NE-SW direction, perpendicular to the regional strike of the main structures. They were spaced 1.5 km apart and tie lines were flown at a spacing of 10 km. A constant clearance altitude of 120 m above the ground level was maintained throughout the survey (Aero Services, 1984). The principal objectives of this work are to make use of the available remote sensing and aeromagnetic data to do the following:

1- To understand the subsurface geology and its relation with the surface geology.

2- To infer accurately the most pronounced tectonic trends (the surface and subsurface) of the study area.

Fig. (1): Location map of Gabal Abu Marwa Area, North Eastern Desert, Egypt.

Various interpretation and analysis techniques are applied to accomplish this task. Reduction to the pole was performed to eliminate the distortion in the magnetic expression associated with the obliquity of the magnetizing field. Trend analysis was performed for magnetic maps, shaded relief and geological map of the study area. Statistical tests are used to manifest the relation between the different data sets. Quantitative interpretation includes modeling approaches and depth estimation using the functions of analytical signal and local wave number

GEOLOGIC SETTING

The regional geologic setting of Gabal Abu Marwa area is mainly illustrated from Schurmann, (1955 and 1966); Said, (1962); Kabesh and Abdel Khalek, (1970); Francis (1972); El-Etr and Abdel Rahman, (1973); El Gaby et al., (1988) and others. The geologic map of the study area (Fig. 2) included within the geologic map of Egypt – NG 36 NE QUSEIR - This map is published in scale 1:500,000 by Conoco Coral and Egyptian General Petroleum Corporation (Klitzsch et al., 1986). The western part of the study area is covered by Precambrian rocks, which are represented by (from oldest) metavolcanics, metagabbro-diorite complex, older granitoids, Dokhan volcanics, Hammamat group and younger granitoids. These rocks are traversed by several wadis (dry valleys) filled with Quaternary alluvial deposits. A long belt of low narrow range hills, which runs parallel to the Red Sea margin, is observed at the eastern part of the study area. This belt represents the southern part of Esh El Milaha range. It rises above the coastal plain to the east, and to the west it is separated by a wide "valley" from the main mass of the Red Sea Hills. This belt consists of small exposures of Precambrian basement rocks and sedimentary rock units of Cretaceous and Tertiary age. The Cretaceous rock units are represented by Nubia group, Duwi Formation and Dakhla Formation. However, the Tertiary rock units are represented by Thebes Formation, Esna Formation and Samih Formation. In general, the area is dissected by a system of faults, most of them trending in the NW-SE (Red Sea) and NE-SW directions (fig. 2).

DATA PROCESSING AND INTERPRETATION

1-Reduction to the North Magnetic Pole (RTP)

Reduction to the pole of magnetic data was used to overcome the inclination problems of intermediate latitudes. In this map (fig. 3), the magnetic anomalies were centered directly above the causative sources. (Baranov, 1957 & 1975; Baranov and Naudy 1964 and Battacharyya, 1965 & 1967).

The RTP map of the study area (fig. 3) is resolved into several closed expressions. Most of these expressions have limited elongation and trending in different directions. A well defined belt trending NW-SE direction is observed at the eastern part of the study area. This belt is associated with Esh El Milaha range and is characterized by positive magnetic anomalies with high amplitude and frequency. Low magnetic relief expressions of relatively long wavelength anomalies are characterizing the sedimentary rock units that covered the western and eastern parts of Esh El Milaha range.

High magnetic closed expressions of relatively short wavelength are observed at scattered locations over the basement outcrop at the western part of the study area. Anomalies of relatively high magnetic contour lines are aligned in a curved shape delineating the eastern boundary of the younger granites. Such relatively high anomalies may be associated with either the granitic rocks of relatively basic nature or a basic material intruded these granitic rocks. Similar intrusions can be assumed to explain the near by -to the west- high contour anomalies. Expressions of the same nature, but of relatively limited wavelength, are observed at scattered locations over the western basement outcrop. Most of these anomalies show positions close to the mapped geological contacts and faults. In general the resolution of the magnetic data into more than one anomaly is observed over the various units of the geological map. This implies the lack of one to one relation between the geological units and its magnetization. However, outstanding magnetic gradient is observed over the contact of some units indicating magnetization contrast higher than that associated with the inhomogeneous susceptibility nature within the geological units itself.

2- Trend Analysis

The term lineament in geology has been applied to imply alignment of different features such as shear zones, faults, rift valley, truncation of outcrops, fold axis, alignment of dikes and elongated pluton, and alignment of stream and valleys (Gupta, 1991). In the present study the structural lineaments were deduced from the analysis of three different data sets (landsat, magnetic and drainage pattern). The significance and tracing criteria for the former lineament types are as follow:

A- Landsat lineaments:

Lineaments in landsat image express different linear geological features. In the present study landsat image data of the study area is transformed into digital elevation model (DEM) in the form of shaded relief image. Lineaments are traced over the shaded relief image (fig. 4)

B- Aeromagnetic lineaments:

Affleck (1963) stated that trend pattern could be used to delineate magnetic provinces, which in turn reflect the tectonic provinces. Gay (1972) specified the following criteria for tracing the aeromagnetic lineaments: 1) - occasional alignments of magnetic lows and/ or highs, 2)- steeping and flatting gradient (changes in gradient), 3)- Termination of highs and lows, and 4)- linear contour pattern. The former criteria can assist in tracing lineaments and can be used individually or in combination. In the present study the magnetic lineaments are traced from the RTP aeromagnetic data.

C- Drainage lineaments:

Drainage lineaments are traced from the geological map of the study area. Tracing is restricted to drainage lineaments of the well-defined trend and appropriate length.

The former lineament trends are grouped into classes according to their azimuth for both lineament number and length. The distributions of the various lineament number and lengths over the azimuth range are divided into 10-degree azimuth classes

Trend correlation is used to summarize the strength relationship between the lineament trends deduced from various data sets. In this regard Spearman's rank correlation coefficient is used as a measure of linear relationship between each pair of the data sets. The data were converted into ranks to measure how tightly the ranked data clusters around a straight line. A positive correlation is one in which the ranks of both variables increase together. Meanwhile a negative correlation is one in which the ranks of one variable increase as the ranks of the other variable decrease. A correlation close to zero means that there is no linear relationship between the ranks (Altman, 1991). The correlation coefficients (rs) and the test of statistical significance (p values) obtained for the various pairs of data sets are illustrated in table (1). This table reflects the following features:

1- Strong correlation is observed between the No% and L% for each pair of the same data type.

2-The correlation coefficient between drainage trends and either landsat or magnetic sets indicates an obvious weak relation.

3- Cases 1, 2 and 3 have p values less than 0.01. This implies a statistical significant relationship at the 99 % confidence level. However cases 4, 5 and 6 have p values less than 0.1, which implies a statistical significant relationship at the 90 % confidence level.

4-The correlation coefficient (0.478) between the landsat and magnetic data is very close to the class of the strong relation. Accordingly it is possible to associate their significance with moderate relationship without much tolerance.

One can notice that statistical test alone is not sufficient to reveal the relation between the data sets. Therefore, the presentation of the lineaments of azimuth distribution (rose diagram) is more convenient to manifest the data sets relation. Rose diagrams (Fig. 5) are prepared to illustrate the relative contribution of these classes for both lineament numbers and lengths. Inspection of the various rose diagrams shows the following:

1- Rose diagram of landsat lineaments (No. %) has peaks in N35°W, N-S, N30°E and N65°E. The order of the former peaks progressively increases toward the west. Rose diagram of the length contribution show similar trend distribution. The observed outstanding lineament relative contribution in the N35°W direction indicates the regional nature of this trend.

2- Rose diagrams of magnetic lineaments (No%) show the main peak at the N35°W direction and secondary peaks at N30°W and N5°W, The rose also includes Third order peaks at N35°E and N65°E directions. The other rose diagram (L%) Show the same trends but with a mutual position of the first pair of trend peak. Also the peaks at the eastern azimuth range have reduced its contribution in comparison to the (No%). The noticed relative increase in the length contribution at some trends implies comparable increase in the regional nature of this trend.

3- Drainage rose diagrams (No % & L %) show a major trend in the NE – SW direction. Secondary and equal order peaks follow the N-S and E–W direction. This outstanding major contribution in the NE – SW direction is due to the contribution of the drainage system associated with Esh El Millaha uplift, which has a NW – SE direction.

Fig. (2): Geologic map of Gabal Abu Marwa area (after Klitzsch, 1986). Symbols are:
Q= Wadi deposits; Tmr= Um Mahara Fm; Ten= Nakheil Fm.; Tpte= Esna Fm.;
Tett= Thebes Fm.; Kud= Dakhla Fm.; Kuw= Duwi Fm.; Kuq= Quseir Fm.
Kutq= Taref Fm.; Pz= Paleozoic rocks; Gy= Younger granite; Go= Older granite
ha= Hammamat sediments; Ms= metasediments; mv= metavolcanics and mgI= metagabbros

Fig. (3): RTP magnetic data and magnetic models profile positions.

Fig. (4) Lineaments traced over shaded relief image of the study area.

In general, the lack of strong relation can be mainly attributed to:

a- The sedimentary exposure units in the landsat images restrict their lineaments contribution to the traced drainage lineaments.

b- The magnetic lineaments are not necessary a surface phenomena meanwhile, geological map and landsat images reveal the surface features.

3- Depth Estimation

Many automatic and graphic techniques have been developed to estimate the depth to the top of source bodies (Grauch and Cordell, 1987; Roest and Pilkington, 1993; Thurston and Smith, 1997; Smith et al., 1998; Abdelrahman and Hassanien, 2000 and others). In order to estimate depths from the grids of magnetic data, some recent techniques require estimations of the magnetic contact locations. This is done by constructing a function from the magnetic data that is peaked over the contacts. Several such functions have been suggested in the literature including the magnitude of the horizontal gradient (Blakely and Simpson, 1986), the amplitude of the analytic signal (Nabighian, 1972; Roest et al., 1992; and Roest and Pilkington, 1993), and the local wavenumber (Thurston and Smith, 1997; and Smith et al., 1998). In each case, the same function that is used to locate the contacts can be used to estimate the source depths at the contact locations. Depths to the top of source bodies have been estimated from the total intensity magnetic data of the concerned area based on the analytic signal and local wavenumber methods that operate on the entire grid of the data. The data processing was carried out utilizing the geophysical software as implemented by Philips (1997).

The depths derived from the analytic signal and local wavenumer are shown in figures 6 and 7 respectively. Reliability of the results with such techniques requires well isolated anomalies and insignificant or well removed noise (Xiong, 2003). In this regard, Upward continuation of the aeromagnetic data grid prior to calculation of the local wavenumber is necessary to minimize data noise associated with the calculation of second derivatives These maps show the relatively deeper nature of the estimation obtained with the local wavenumber technique in comparison to those obtained with the analytic signal approach. However the two maps show a basin of a NW-SE direction parallel to the Red Sea. The basin is bounded from the east and west by shallower depth values, where these parts are covered by basement rocks. The basin has irregular shape with deeper parts at the central portion. The basin configuration and boundaries in both maps manifst the impact of NW-SE, N-S and NE-SW fault trends. Right lateral movement along the NE-SW direction is revealed in the analytic signal depth estimation map.

4- Magnetic Modeling

Geophysical inversion can be considered as an attempt to fit the response of a subsurface earth model to a finite set of actual observations. The model parameters and model response are the main primary elements in the inversion process. In this regard, the model consists of a set of mathematical relations representing a particular mathematical description of an observed process. In a modeling technique, a specific fixed geometric model could be used to calculate the depth, width, location and magnetization of the source of a magnetic anomaly. The computed magnetic anomaly of the entire model along the profile is the sum of the contributions of each separate polygon. The data processing was carried out using GM-SYS modeling software, included in the OASIS Montaj Data Processing and Analysis System (1997).

In the present study, 42 magnetic profiles were selected in the modeling process (Fig. 3). Some of these models (M6, M7, M17, M20, M24, M25, M30, M35, M38, M40, M41 and M42) were selected for illustration and discussion (figs 8 to 10).

Over the acidic metavolcanic units, four models (M6, M7, M17 and M20) have been carried out (Fig. 8). These rock units show relatively low magnetization due to their limited thickness and low magnetic susceptibility values. The first model (M6) includes distribution of materials that have limited depth extension and low magnetic susceptibility at the top. These materials represent the distribution of the acidic metavolcanics. This unit overlies rock units of relatively high susceptibility contrast in the middle portion, hosted laterally with materials of lower susceptibility values. The second model (M7) has been constructed over the metavolcanic and younger granite. This model reveals the distribution of the acidic metavolcanic at the top with maximum depth extension of 1200 m, and basement units of different susceptibilities (0.005, 0.000156 and 0.0078 cgs). The metavolcanic partially overlies the first and the second units. The third model (M17) exhibits the metavolcanic overburden with depth extension varies from 400m to 2000m. The metavolcanic capped materials at the central portion of magnetic susceptibility of 0.0019 cgs. These materials are hosted by rock units of relatively low susceptibility. The forth model (M 20) shows the depth extension of the metavolcanic units varying from 500 m to 1400 m. This model shows changes in the susceptibility contrast values of the underlying units.

Figure (9) shows four modeling profiles (M24, M25, M30 and M35) that were selected over different rock units. The first model (M24) has been constructed over the older granite which shows diversity of susceptibility contrast values for the model blocks (0.0018, 0.0002 and 0.001 cgs). The second model (M25) was selected over metagabbro rock unit.

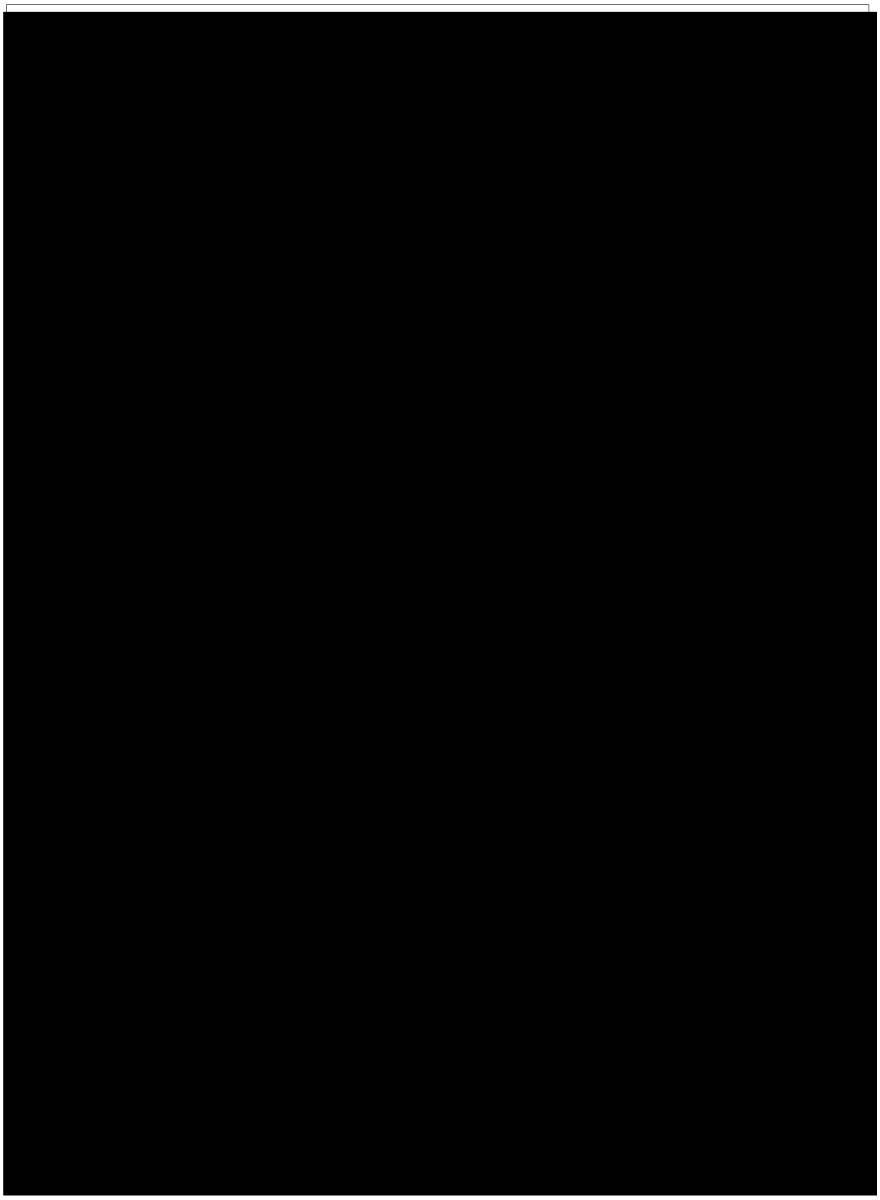

Fig (5): Rose diagrams (Number % & length %) for the different data sets (landsat, magnetic and drainage lineaments)

Fig. (6): Depth estimation contour map to the top of source bodies, as deduced from the analytic signal. Dashed lines indicate possible fault locations and arrows indicate possible right latera displacement

Fig. (7): Depth estimation contour map to the top of source bodies, as deduced from the local wavenumber. Dashed lines indicate possible fault locations.

Fig. (8): Magnetic modeling along profiles Nos. 6, 7, 17, and 20.

Fig. (9): Magnetic modeling along profiles Nos. 24, 25, 30 and 35.

It exhibits low susceptibility and rootless nature of this unit with depth extension of about 1300 m and lying over basement rock units of relatively high magnetization contrast. Such low value is not expected for metagabbro. Profile model (M30) was taken over the Dokhan volcanic, which reflects variation from 400 to 1450 m in the thickness of the Dokhan volcanic. Low magnetic susceptibility value has been assigned to Dokhan volcanic. Also, the model shows diversity in the magnetization of the basement rock units that underlying the Dokhan volcanic. The extremely high susceptibility contrasts observed in the underlying material are associated with one of the relatively high magnetic anomalies that are scattered over the basement rock units. At the eastern part of the study area, the model expressed the Dokhan exposure as a cap unit of relatively low susceptibility contrast (0.00003 cgs) overlaying blocks of different contrasts. Extremely high contrast (0.0025 cgs) is observed in the middle portion of the model beneath the cap rock. Model (M35) profile extends, from west to east, over the sedimentary, Dokhan volcanic, Hammamat sediments and sedimentary exposures respectively. The model express these units with low magnetic susceptibility values and depth extension vary from 200 m to 1400 m at the east. The sediments are expressed in the top model with zero magnetization and maximum depth extension of 1600m. Beneath the top layer, basement units of dramatic diversity in magnetization nature are observed, which are varying from low magnetization (0.0001 cgs) to extremely high magnetization (0.0073 cgs).

Model (M38) has been carried out for magnetic profile extends over the sediments outcrops between the western basement outcrop and Esh El Millaha at the east (Fig.10). In this model the magnetically transparent sediment is observed over basement blocks of different susceptibility contrasts. At Gabal Abu Shar El Qeply two models (M40 and M41) have been constructed (Fig.10), which show similar pattern of the subsurface distributions. Both models show transparent magnetic materials at the top, which expresses sedimentary cover. Both models show decreasing of the sedimentary thickness in the central part, which is associated with the basement uplift that has relatively high magnetic contrast (0.00185 and 0.0018 cgs). The thickness of the sediment varies from 100 m to 900 m over the central uplift. This uplift is an extension of Esh El Milaha range, which expose north Gabel Abu Shar El Qeply. Model (M42) indicates shallow sediments in the western part and the thickness of these sediments has a maximum value at the middle portion of the profile (Fig.10). It gradually decreases toward the basement outcrops. The later models suggest possible control of the basement block uplifts on the configuration of the overlying sediments. The fault block geometry of such structural pattern for the southern part of the Gulf of Suez at the early pahse of rift is illustrated in figure (11) as interpreted by Bosworth (2005).

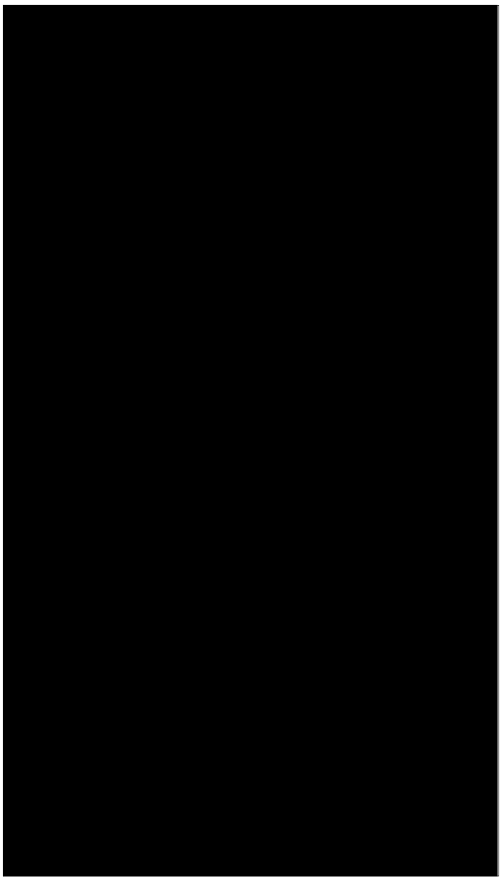

Fig. (10): Magnetic modeling along profiles Nos. 38, 40, 41 and 42.

The parameters (Susceptibility contrast, depth and width) values of the all models (43 models) are illustrated in table 2. The relation between the main parameters is manifested in Figure. (12). The top units of the former models express near surface material distribution. The parameters of the top units are not included in the former table. The depth extension and susceptibility contrast values of the top unit group are shown in table (3). The inspection of the obtained results of the frequency histograms (fig. 13) that illustrating the parameters of near-surface rock units shows:

1- Near surface units have limited depth extension and low suscebtibilty contrast values

2- The susceptibility values range from 0.000001 cgs to 0.0072 cgs unit. Most of the former values are less than 0 .022 cgs units

2- The depth to the magnetic sources bodies is ranging from 0 m to 1400 m.

3- The width value is ranging from 100 to 7000 m and most of the thickness values do not exceed 4000 m.

4- There is no obvious relation between any pair of the former parameters.

Fig. (11): Cross-section across the souther part of the Gulf of Suez, illustrating rotated fault block geometry that is throught to be representative of the early phases of Red Sea rifting (after Bosworth, et al., 2005)

Fig. (12): Relation between depth, width and magnetic susceptibility for the selected profile models

Fig. (13): Susceptibility and depth extension of the near surface rock units (top units)

Table (1): The correlation coefficients (rs) and test of the statistical significance (p values) for the various data pairs

Serial No.	Case	Spearman correlation coefficient (Rs)	P value
1	landsat lineaments (No%) & landsat lineaments. (L%)	0.72	.0007
2	magnetic lineaments (No%) & magnetic lineaments. (L%)	0.98	0.0
3	drainage (No%) & drainage lineaments.(L%)	0.9	0.0
4	Landsat lineaments (No%) & magnetic lineaments. (No%)	0.478	.051
5	landsat lineaments (No%) & drainage lineaments. (No%)	0.049	.078
6	magnetic lineaments (No%) & drainage lineaments. (No%)	0.11	.074

Table (2): The main parameters (Susceptibility contrast, depth and width) of the selected profiles.

M no	sus. (cgs)	Depth (m)	Width (m)	M no	sus. (cgs)	Depth (m)	Width (m)	M no	sus. (cgs)	Depth (m)	Width (m)
1	0.0008	200	2200	18	0.00003	300	950		1E-06	640	1500
2	0.002	0	3100		0.0023	300	1300	34	0.0019	430	1700
3	0.0021	0	3300	19	0.0025	130	2600	35	0.0012	100	5200
	8E-06	0	1500	20	0.00002	0	800		0.007	900	6500
4	1E-05	0	2000		0.0012	400	2300		0.005	900	2000
	0.0013		2500	21	0.0002	340	1500	36	0.001	0	2000
	0.0013	0	1300	22	0.000001	1150	6000		0.0005	600	700
5	0.0028	0	2000	23	0.00023	300	3000		0.0008	1000	2000
	0.0008	0	2800		0.00001	500	1200	37	0.0025	0	6500
	0.0008	0	3100	24	0.001	300	1400	38	0.0037	0	1600
6	0.0011	140	2500		0.000001	0	1600		0.0072	0	800
7	0.0013	0	1700	25	0.00195	1100	1500		0.0015	0	1400
	0.0007	0	1500		0.0000`	1000	1000		0.0066	0	700
	0.0005	0	2500		0.0004	700	1700		0.0001	0	250
8	0.001	0	2300	26	0.0012	0	1300		0.0001	0	460
9	0.0014	0	1100		0.0014	0	2000		0.0015	0	600
	0.001	0	850	27	0.0026	400	3200		0.0072	0	100
	0.001	0	2200		0.0001	300	850	39	0.0003	300	1900
10	0.0029	0	1700		0.00001	280	800		0.0001	0	2200
	0.0008	0	2200	28	0.00126	0	4000	40	0.0019	0	5300
11	1E-05	0	1100		0.00016	500	1300		0.0001	350	1200
12	1E-06	0	700	29	0.0011	700	3000	41	0.0019	0	5400
13	0.0013	0	2800	30	0.0028	600	4500	42	0.0004	0	800
14	0.0025	0	2600		0.00004	700	600		0.0014	700	7000
15	0.0022	0	1800	31	0.0007	0	1500	43	0.0001	1400	4800
16	0.0002	0	1800		0.0003	0	1400		0.0035	100	9800
	0.0011	0	2200	32	0.0015	240	1150		0.0004	1200	9000
	0.0011	0	1800	33	0.0025	200	600		0.0012	1000	2000
17	0.0013	0	3000		0.0007	200	600		0.0015	1300	5000

Table (3): The main parameters of the top rock units of the different models.

Model No.	**Sus. (cgs)**	**Depth (m)**	**Model No.**	**Sus. (cgs)**	**Depth (m)**
1	0.00001	1160	28	0.000047	1100
2	0.00001	770	29	0.00001	1480
5	0.00001	900	30	0.00002	1500
6	0.000012	950	32	0.000028	375
8	0.00001	1060	33	0.00003	810
9	0.000011	680	34	0.00003	980
10	0.0001	700	35	0	1300
11	0.0001	700		0.000032	540
14	0.0001	820		0	1450
16	0.0011	600	36	0.00001	1600
17	0.000042	1200		0.0002	1150
19	0.00001	1200	37	0	2200
20	0.00004	1400	38	0.0001	660
21	0.00004	700	39	0	600
22	0.00001	1100	40	0	900
23	0.0001	770	41	0	700
24	0.00001	500	42	0	1000
26	0	600	43	0	1300
27	0.00001	1000			

CONCLUSIONS

The analysis of the available Landsat and aeromagnetic data of the study area, aided by the geologic information, revealed the following:

1- Lack of one to one relation between the various geological units and the magnetic anomaly is observed due to diversity in the magnetization of these units.

2- Lineament analysis of the different data sets reveals four predominant sets of structural lineaments trending mainly in the NW-SE, N-S, NE-SW and E-W directions. Diversity in correlation strength and is observed between the different data sets.

3- The magnetic basement depth estimation maps show irregular surface configuration with an obvious basin trending NW-SE direction. A right lateral movement is observed in the former basin configuration.

4- At Gabal Abu Shar, the subsurface basement configuration suggests an extension of Esh El Milaha range.

5- Metavolcnics, dokhan volcanics and metagabbro intrusive units have limited depth extension with low susceptibility values assuming acidic nature for these

REFERENCES

Abdelrahman, E.M. and Hassanien, H.I., (2000): Shape and depth solutions from magnetic data using a parametric relationship, Geophysics Vol. 52, P. 126-131.

Aero Services, (1984): "Interpretation report of airborne gamma – ray spectrometer and magnetometer survey of the Eastern Desert of Egypt". pp.1-127.

Affleck, J., (1963): Magnetic anomaly trend and spacing patterns, Geophys. V. 28, No. 3, pp 379-395.

Altman D.G. (1991): Practical Statistics for Medical Research. Chapman & Hall, London, pp. 285-288. From Blackwell Science Ltd, Journal of Clinical Nursing (1999), 8, 762-763.

Baranov, V., (1957): A new method for interpretation of aeromagnetic maps: pseudo-gravimetric anomalies: Geophysics, V. XXII, No. 2, pp. 359-383.

Baranov, V. and Naudy, H., (1964): Numerical calculation of the formula of reduction to the magnetic pole: Geophysics, V. XXIX, No. 1, pp. 67-79.

Baranov, V. (1975): Potential fields and their transformations in applied geophysics: Geoexploration Monographs, Serier L, No. 6, Gebruder Borntrager, Berlin, Stuttgart, Germany.

Battacharyya, B.K., (1965): Two-dimensional harmonic analysis as a tool for magnetic interpretation. Geophys., V. 30, pp 829-857.

Battacharyya, B.K., (1967): Reduction filter for digital processing of potential field data. Geophys., V. 32, pp 712-726.

Blakely, R.J., and Simpson, R.W., (1986): Approximating edges of source bodies from magnetic or gravity anomalies: Geophysics, V.51, No.7, p.1494-1498.

Bosworth, W., Huchon, P. and McClay, K. (2005): The Red Sea and Gulf of Aden Basins, Journal of African Earth Sciences. 43, 334–378.

El-Etr, H.A., and Abdel Rahman, M.A. (1973): Drainage pattern and drainage lineations of Esh El Mellaha Range, Gulf of Suez District, Egypt: 7th, Arab. Sci., Congr. Bull, Cairo, Egypt. V.1, pp.265-282.

El Gaby, S., List, F.K., and Tehrani, R. (1988): Geology, evaluation and metallogenesis of the Pan-African Belt in Egypt, in the Pan-African Belt of Northeast African and adjacent areas. Ed. By S. El Gaby and Greilling, pp. 17-68, Friedr. Viewey, Braunsch weig, Federal Republic of Germany.

Erdas Imagine V 8.7: Leica Geosystems GIS & Mapping, LLC., 2801 Buford Highway Atlanta, Georgia 30329, USA.

Francis, M.H., (1972): Geology of the basement rocks in the northern Eastern Desert between latitudes 27 30 and 28 00 N. Annals Geologic Survey of Egypt 2, pp161-180.

Gay, S.P.,(1972): The new basement map, fundamental characteristics of aeromagnetic lineaments, their geological significant to geology, American Stereo Map Company, Salt Lake City, Utah.

Grauch, V.J.S., and Cordell, L., (1987): Limitation on determining density or magnetic boundaries from horizontal gradient of gravity or pseudogravity data: Geophysics, V. 52, No.1, p.118-121.

Gupta, A.P., (1991): Remote Sensing geology. 356. PP, Berlin-Heidlberg (springer).

Kabesh, K.L. and Abdel Khalek, M.L. (1970): Petrochemical characters of Wadi El Mellaha granitic rocks, Esh El Mellaha Range, Eastern Desert, Egypt: J. Geol., V.14, No.1, pp. 1-12.

Klitzsch, E., F.K. List and G. Pöhlmann, (1986): Geological map of Egypt (1:500,000 in 20 sheets): Conoco Coral and Egyptian General Petroleum Corporation (Cairo).

Nabighian, M.N., (1972): The analytic signal of two-dimensional magnetic bodies with polygonal cross-section: its properties and use for automated anomaly interpretation: Geophysics, V.37, No.3, pp.507-517.

Phillips, J.D., (1997): Potential-field geophysical software for the PC, version 2.2: U.S. Geological Survey Open-File Report 97-725, 34p.).

Roest, W.R., Verhoef, J. and Pilkington, M. (1992): Magnetic interpretation using the 3D analytic signal, Geophys. V. 57, pp 16-125.

Roest, W.R., and Pilkington, M., (1993): Identifying remanent magnetization effects in magnetic data: Geophysics, V.58, No.5, pp.653-659.

Smith, R.S., Thurston, J.B., Dai, T., and MacLeod, I.N., (1998): ISPI- the improved source parameter imaging method: Geophysical Prospecting, V.46, pp.141-151.

Said, R. (1962): The geology of Egypt. 377 p, 10 pls. Elsevier. Amsterdam, London, New York.

Schurmann, H.M.E. (1955): The Precambrian History of the Gulf of Suez area, Bull., Soc. Geol., Cairo, Egypt. V. 45, pp. 170-193.

Schurmann, H. M. E. (1966): The Precambrian along the Gulf of Suez and the northern part of the Red Sea, Leiden, E. J. Berl., Netherlands, 40 p.

Thurston, J.B., and Smith, R.S., (1997): Automatic conversion of magnetic data to depth, dip, and susceptibility contrast using the SPI method: Geophysics, V.62, No.3, pp.807-813.

Xiong L., (2003): On the use of different methods for estimating magnetic depth, the leading edge volume 22 issue 11 pp. 1090-1099.